PYCR2 Mutations Cause a Lethal Syndrome of Microcephaly and Failure to Thrive

Maha S. Zaki, MD, PhD,[1] Gifty Bhat, MD,[2,3] Tipu Sultan, MD,[4]
Mahmoud Issa, MD, PhD,[1] Hea-Jin Jung, PhD,[2] Esra Dikoglu, MD, PhD,[2]
Laila Selim, MD,[5] Imam G. Mahmoud, MD, PhD,[5]
Mohamed S. Abdel-Hamid, MD,[6] Ghada Abdel-Salam, MD, PhD,[1]
Isaac Marin-Valencia, MD, MS,[2] and Joseph G. Gleeson, MD[2]

Objective: A study was undertaken to characterize the clinical features of the newly described hypomyelinating leukodystrophy type 10 with microcephaly. This is an autosomal recessive disorder mapped to chromosome 1q42.12 due to mutations in the *PYCR2* gene, encoding an enzyme involved in proline synthesis in mitochondria.
Methods: From several international clinics, 11 consanguineous families were identified with *PYCR2* mutations by whole exome or targeted sequencing, with detailed clinical and radiological phenotyping. Selective mutations from patients were tested for effect on protein function.
Results: The characteristic clinical presentation of patients with *PYCR2* mutations included failure to thrive, microcephaly, craniofacial dysmorphism, progressive psychomotor disability, hyperkinetic movements, and axial hypotonia with variable appendicular spasticity. Patients did not survive beyond the first decade of life. Brain magnetic resonance imaging showed global brain atrophy and white matter T2 hyperintensities. Routine serum metabolic profiles were unremarkable. Both nonsense and missense mutations were identified, which impaired protein multimerization.
Interpretation: *PYCR2*-related syndrome represents a clinically recognizable condition in which *PYCR2* mutations lead to protein dysfunction, not detectable on routine biochemical assessments. Mutations predict a poor outcome, probably as a result of impaired mitochondrial function.

ANN NEUROL 2016;80:59–70

Proline is a nonessential amino acid involved in protein biosynthesis and antioxidant reactions.[1,2] It is endogenously synthesized from glutamate via pyrroline-5-carboxylate synthase (P5CS), which converts glutamate to pyrroline-5-carboxylate (P5C). P5C can be converted to proline by 1 of 3 paralogues in mammals: PYCR1, PYCR2, and PYCRL, linked to the group of rare PYCR-related disorders (Fig 1A). Defects of proline synthesis have major deleterious effects on health, leading to intellectual disability,[2–4] skin and joint hyperelasticity, osteopenia,[5,6] and cataracts.[7]

The clinical and molecular phenotype of disorders of proline synthesis is currently under intensive investigation. To date, mutations only in *PYCR1* (Online Mendelian Inheritance in Man [OMIM] 616406) and *PYCR2* (OMIM 179035) have been associated with human

View this article online at wileyonlinelibrary.com. DOI: 10.1002/ana.24678

Received Jan 12, 2016, and in revised form Mar 18, 2016. Accepted for publication Apr 17, 2016.

Address correspondence to Dr Gleeson, Laboratory for Pediatric Brain Disease, Howard Hughes Medical Institute, Rockefeller University, New York, NY 10065. E-mail: jogleeson@rockefeller.edu

From the [1]Human Genetics and Genome Research Division, Clinical Genetics Department, National Research Center, Cairo, Egypt; [2]Laboratory for Pediatric Brain Disease, Howard Hughes Medical Institute, Rockefeller University, New York, NY; [3]Division of Pediatric Genetics, Children's Hospital at Montefiore, Bronx, NY; [4]Pediatric Neurology, Institute of Child Health, Children Hospital, Lahore, Pakistan; [5]Cairo University Children's Hospital, Division of Neurology and Metabolic Disease, Cairo, Egypt; and [6]Department of Medical Molecular Genetics, Human Genetics and Genome Research Division,
National Research Center, Cairo, Egypt.

Additional supporting information can be found in the online version of this article.

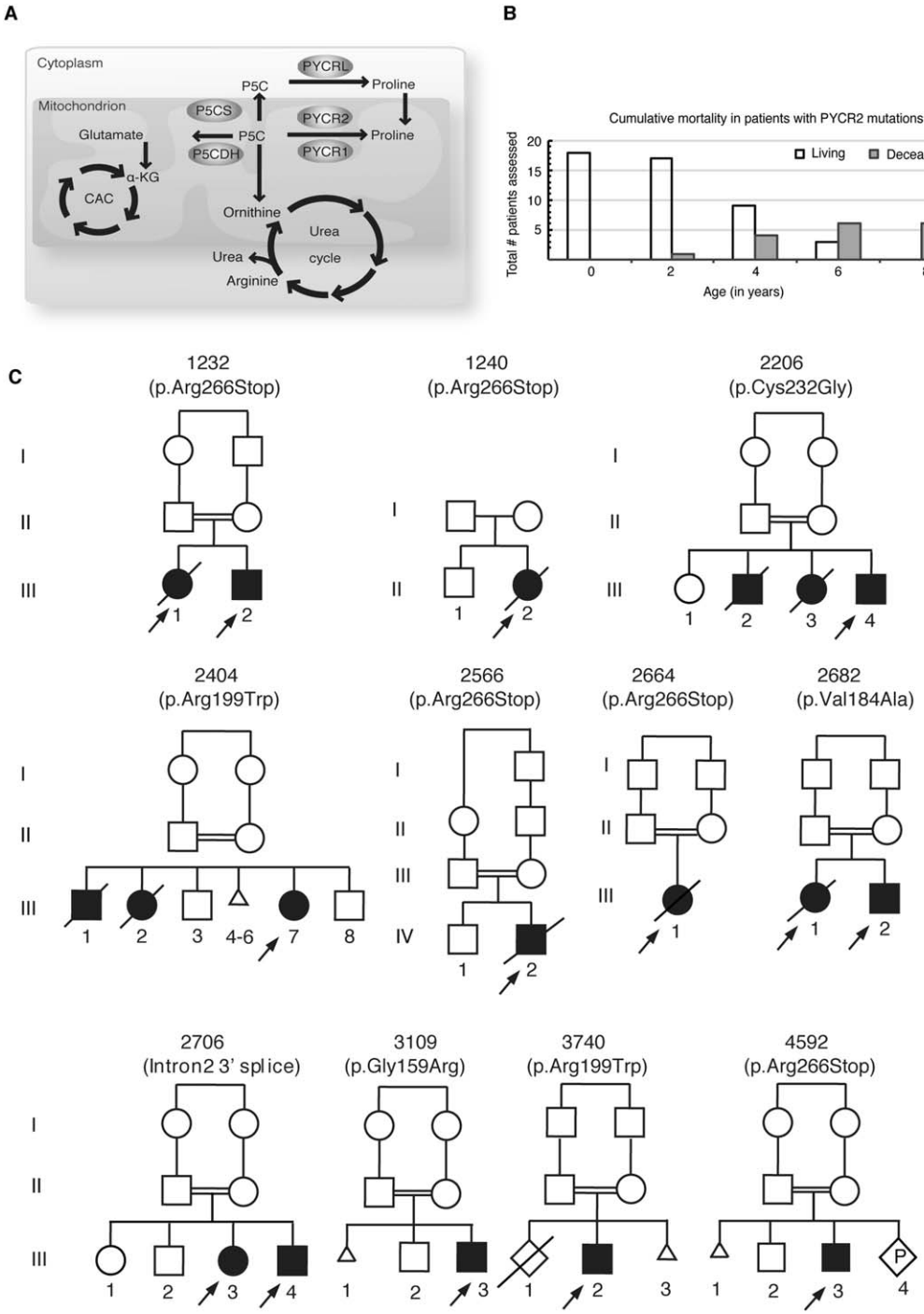

FIGURE 1: Overview of proline metabolism and individuals with *PCYR2* mutations. (A) Pyrroline-5-carboxylate reductase 2 (PYCR2) functions in the mitochondria with the paralogue PYCR1 for conversion of pyrroline-5-carboxylate (P5C) to proline. P5C can also be converted to proline in the cytoplasm, mediated by PYCR-like (PYCRL). P5C can alternatively be used as a substrate for ornithine synthesis, which can enter the urea cycle, or can be interconverted to glutamate, mediated by pyrroline-5-carboxylate dehydrogenase (P5CDH). Glutamate can then be used as a substrate for the citric acid cycle (CAC) or can be converted back to P5C by pyrroline-5-carboxylate synthetase (P5CS). (B) Bar diagram depicting cumulative survival of the 18 subjects, including 14 study patients, as well as 4 deceased siblings with similar clinical presentation at the time of ascertainment. The white bars represent the living and gray bars represent the deceased individuals at any given age interval. By age 8 years, 9 individuals (5 study patients and 4 siblings) had died; there are no living survivors beyond 10 years of age. (C) Pedigree diagrams showing 11 families, with a total of 18 individuals who displayed features of neurodevelopmental delay; 14 children were recruited for the study and found to have homozygous mutations in *PYCR2*. All pedigrees but 1240 had documented parental consanguinity *(double bar)*, either first-cousin once removed (2566) or first cousin (all others). Generation number and individual family IDs are labeled. Arrows = probands in each family with *PYCR2* mutation, filled symbols = affected subjects, squares = males, circles = females, hashed = deceased, triangles = miscarriage. P = proband.

disease. Homozygous mutations in *PYCR1* were reported in families presenting with cutis laxa and progeroid features.[8,9] Fibroblasts from patients showed defective mitochondrial morphology, reduced mitochondrial membrane potential, and a 5-fold increase in apoptosis upon oxidative stress.[9] Proline levels in plasma were normal. Mutations in *PYCR2* were recently reported in 2 consanguineous families with microcephaly and cerebral hypomyelination.[10] Similar to patients with *PYCR1* mutations,[8] no evidence for proline depletion was found in patient serum, suggesting functional redundancy of multiple PYCR paralogues in proline production. *PYCR2*-related disorder has been classified as hypomyelinating leukodystrophy-10 (OMIM 616420) based on the report of these 2 families.

Here, we expand the clinical account of *PYCR2*-related disorders by presenting 14 patients from 11 consanguineous families with homozygous *PYCR2* mutations. The clinical phenotype was remarkably consistent between patients, characterized by microcephaly (occipitofrontal circumference of 3–6 standard deviations [SD] below the mean), severe psychomotor delay, failure to thrive, facial dysmorphism, and white matter hyperintensities with global brain atrophy on magnetic resonance imaging (MRI). Intellectual and motor functions worsened over time, and none of the patients survived beyond the first decade of life. Mutations clustered in the dimerization domain of the protein, and several tested mutations impaired multimerization. We propose that *PYCR2*-related disorder is a clinically recognizable lethal genetic leukoencephalopathy syndrome without biochemical alterations on standard clinical assays.

Subjects and Methods

Patient Material

We recruited subjects to this study as part of an assessment of children with neurodevelopmental disorders presenting to clinics in regions of the world displaying elevated rates of parental consanguinity. The total cohort includes >5,100 individual families and 9,400 participants recruited between the period of 2004–2015 presenting with features of intellectual disability, autism-related conditions, microcephaly, structural brain disorders, epilepsy, or neurodegeneration. The cohort was enriched for families with recessive pediatric brain disorders with homozygous mutations, due to documented consanguinity in >80% of pedigrees and multiple affected members in 63% of families. General physical and neurological examinations as well as evaluation of brain MRI or computed tomography (CT) were carried out as part of the standard clinic evaluation. Pedigree analysis and blood sampling were pursued in all families, and subjects were selected for exome sequencing based upon a clinically defined neurodevelopmental genetic condition.

The study included 11 families, (family ID 1232, 1240, 2206, 2404, 2566, 2664, 2682, 2706, 3109, 3740, and 4592) with 14 affected members with pediatric onset neurological features and autosomal recessive inheritance. Two families (2206 and 2404) had 2 diseased siblings each who presented identically to the ascertained probands, but were deceased prior to ascertainment. None of the families has been previously reported. All patients were examined by at least 1 of the authors, and clinical details including videos were recorded at the time of each visit. The study was approved by the ethical committees of participating institutions, and all ascertainment was performed with informed consent.

Genotyping

Genomic DNA was extracted from blood leukocytes or saliva samples by standard methods from all genetically informative members wherever possible, to include parents, and affected and unaffected offspring. The extracted DNA samples were tested for quality and family integrity with a panel of fluorescent genotyping markers using polymerase chain reaction and analyzed using an ABI 3130xl automatic DNA Genetic Analyzer and ABI Peak Scanner Software v1.0 (Applied Biosystems, Foster City, CA).

Whole Exome Sequencing

Five hundred nanograms of genomic DNA were subjected to whole exome sequencing (WES), using Agilent (Santa Clara, CA) Sure Select Human All Exome 50Mb reagents and the Illumina (San Diego, CA) HiSeq 2000 platform 150bp paired-end sequencing, resulting in >100× average exon coverage. Exomes were aligned to hg19 reference genome, and variants were identified using the GATK Toolkit,[11] annotated and prioritized using custom Python scripts.[12]

Sanger Sequencing

Potential disease-causing variants identified from WES were validated and tested for segregation using fluorescent Sanger sequencing. Each member of the family for whom DNA was available was tested for zygosity. Allele frequencies were determined from the ExAC data set and from an in-house 5000 WES library of geographically similar individuals. Sequences were analyzed with Sequencher 5.1 software (Gene Codes Corporation, Ann Arbor, MI).

Skin Cell Isolation and Culture

Skin biopsies were performed on patients and unaffected available family members following informed consent. Mutant and control fibroblasts were generated from explants of dermal biopsies and tested negative for mycoplasma prior to study. Primary skin fibroblasts were cultured in minimal essential medium (Gibco, Grand Island, NY) supplemented with 20% FBS (Gemini Bio Products, West Sacramento, CA) and penicillin as previously reported.[13] All experiments were performed with fibroblasts at passage 5–8.

Cell Transfection and Coimmunoprecipitation

The wild-type human *PYCR1*, *PYCR2*, and *PYCRL* were amplified from mammalian gene collection (MGC) fully sequenced

cDNA clones (*PYCR1*, IMAGE:3505512; *PYCR2*, IMAGE:2901360; *PYCRL*, IMAGE:3533609; GE Dharmacon, Lafayette, CO), cloned into either FLAG- or Myc/His-tagged mammalian expression vectors, and mutagenized to incorporate patient mutations. 293T cells (ATTC, Manassas, VA) were cotransfected with the FLAG- or Myc/His-tagged expression vectors using Lipofectamine 2000 (Thermo Fisher Scientific, Waltham, MA), and cell extracts were used for coimmunoprecipitation with anti-Flag M2 affinity gel (Sigma, St Louis, MO). Input and output samples were analyzed by Western blotting with primary antibodies against PYCR1 (Protein Tech, Rosemont, IL; 13108-1-AP), PYCR2 (Sigma, HPA056873), PYCRL (Novus Biological, Littleton, CO; H00065263-M01), FLAG (Sigma, F7425), c-Myc (Santa Cruz Biotechnology, Dallas, TX; sc-40), 6X His (GeneTex, Irvine, CA; GTX30500), or α-tubulin (Sigma, T6074), detected by horseradish peroxidase–conjugated secondary antibodies and chemiluminescence (Thermo Fisher Scientific).

Results

Identification of Mutations in PYCR2

We sequenced 2 affected individuals in multiplex families, or 1 affected and both parents in simplex families. Analysis of Family 1232 led to the identification of homozygous nonsense mutations in *PYCR2*, which then prompted a search of our exome database, identifying 6 additional families (1240, 2206, 2404, 2566, 2664 and 2682) with *PYCR2* mutations. Once the clinical features were clarified, additionally 4 families were identified with *PYCR2* mutations from clinics (2706, 3109, 3740, 4592) by direct Sanger sequencing. Only 1 family where presenting features matched the *PYCR2* phenotype was negative for *PYCR2* mutation, and this family is still under investigation. In total, 11 families displayed convincing homozygous mutations, and clinical features for all were uniformly similar. No other homozygous variants in *PYCR2* met criteria for causation (<0.1% allele frequency, Genomic Evolutionary Rate Profiling score > 4.5, homozygous in all affected sequenced) in any other families, irrespective of the clinical presentation. Mutations included introduction of a stop codon (p.Arg266-Stop shared by 5 families), substitution of highly conserved amino acids (p.Cys232Gly, p.Arg199Trp shared by 2 families, or p.Val184Ala, p.Gly159Arg), and splice site mutation (3′ splice site of intron 2). Direct questioning showed no evidence of shared ancestry for families sharing a common mutation. No correlation was detected between individual mutation and disease severity. No biases were detected in severity or age of onset based upon patient sex, and all mutations were fully penetrant without observed phenocopies within the family.

TABLE. Summarized Clinical Features of Patients with *PYCR2* Mutations

Clinical Finding	Patients, %
Microcephaly	100% (14 of 14)
Failure to thrive	100% (14 of 14)
Excessive vomiting	29% (4 of 14)
Facial findings	
Typical facies: malar hypoplasia, upturned bulbous nose, low-set prominent ears	100% (14 of 14)
Triangular face	86% (12 of 14)
Neurological findings	
Global developmental delay	100% (14 of 14)
Intellectual disability	100% (14 of 14)
Upper motor neuron signs	100% (14 of 14)
Ataxia or absent gait	100% (14 of 14)
Hyperkinetic movements	100% (14 of 14)
Muscle atrophy	93% (13 of 14)
Seizures	57% (8 of 14)
Spasticity	57% (8 of 14)
Nystagmus	21% (3 of 14)
Brain imaging findings	
Cortical atrophy	100% (13 of 13)
Thin corpus callosum	61% (8 of 13)

Clinical Features of the Affected Individuals

BIRTH HISTORY. Clinical features of the 14 affected individuals are summarized in the Table, and reported in detail in the Supplementary Table. All families were of Egyptian origin, except for Family 2706, which was Pakistani. Parental consanguinity was present in all families except Family 1240 (see Fig 1C). The study included 7 females and 7 males, and ages ranged from 4 months to 6 years. All patients were born full term without complications during pregnancy and delivery. Measurements at birth including weight and height were in the normal range. Head circumference at birth was available in 10 of 14 patients and ranged from 1.8 to 3 SD below the mean (see Supplementary Table).

CHILDHOOD PRESENTATION. Patients presented with profound psychomotor delay, microcephaly, truncal hypotonia with variable appendicular spasticity, and

failure to thrive from the ages of 2 months to 1 year. All stagnated at the developmental level of a 4- to 5-month old infant. They were able to achieve some head control and visual tracking, and could recognize family members, and some were able to sit with support (Patients 2682-III-1, 2682-III-2). None developed meaningful language or fine motor skills, and none was able to stand or walk independently. Primitive neonatal reflexes such as grasp and sucking reflex were seen in those more severely affected (Patient 3740-III-2), even after age 2 to 3 years. Seizures were seen in 57% of patients with onset usually before 1 year of age, consisting of focal myoclonic and generalized tonic–clonic seizures, controlled with anticonvulsant medications. Excessive vomiting of unknown etiology was seen in 29% of patients (Patients 1232-III-1, 1232-IV-2, 1240-II-2, and 4592-III-3), with onset at about 1 to 2 months of age. Audiology evaluation, wherever available, showed bilateral mild to severe hearing loss. Serial clinical follow-up demonstrated progression of symptoms in patients. Families 2206 and 2404 had 2 siblings each (not included in this study) with a similar clinical presentation and early death. Patients 1232-III-1, 1240-II-2, 2566-IV-2, 2664-III-1, and 2682-III-1 died at or before age 6 years due to complications of pulmonary infection, fever of unknown origin, and/or failure to thrive, and no patient survived beyond age 10 years (see Fig 1B).

EXAMINATION. Although all individuals were born with average growth parameters, failure to thrive was noted by 1 year of age. Head circumference was 3 to 6 SD below the mean, height was 2 to 5 SD below the mean, and weight was 4 to 9 SD below the mean. A characteristic craniofacial dysmorphism was noted in most of the patients, which included triangular facies, malar hypoplasia, large malformed ears with overfolded helices, upturned nose with bulbous tip, and a long smooth philtrum (Fig 2). Additional facial features of hypertrichosis and full lips were noted in 4 patients. Bitemporal narrowing due to severe microcephaly was noted in less than half of the patients. Skeletal features of long thin fingers and toes were observed in 4 patients, and 2 had pectus carinatum. Family 1232 (Patients 1232-III-1 and 1232-III-2) demonstrated a slightly different facial gestalt compared to the other patients including synorphrys, prominent glabella, short forehead, gum hyperplasia, arched narrow palate, and dental malocclusion.

On examination, patients were awake and alert to the environment, and none was verbal. Nystagmus was noted in 21% of patients, commonly manifested as slow horizontal and symmetric eye movements in both directions. Truncal hypotonia with hyperreflexia was seen in most patients. Mild to severe appendicular spasticity was present in 57%. Muscle atrophy was evident in all except Patient 1232-III-2. The majority of patients demonstrated hyperkinetic movements of upper and lower extremities, along with spontaneous mouth chewing and head titubation (Supplementary Video).

MRI FEATURES AND BIOCHEMICAL INVESTIGATION. Brain imaging (Fig 3) was available in 13 of the 14 subjects. Six of 14 patients underwent CT head imaging, whereas others had MRI. Some patients showed severe cerebral atrophy (Patients 2404-III-7, 3740-III-2) with ventriculomegaly, in contrast to other patients in whom atrophy was less severe. Thin corpus callosum was seen in 61% of patients. Overall, cerebellum and brainstem were preserved except in Patients 2706-III-3 and 2706-III-4. Metabolic profile, including serum creatinine, blood urea nitrogen, creatine phosphokinase, ammonia, lactate, plasma amino acids, and urine organic acids, was normal in all patients. Urine amino acids were available in 2 families (2206 and 2664), which showed mildly elevated glutamate levels at 84 and 109nmol/mg creatinine (reference level $<$ 76nmol/mg creatinine), respectively, compared to unaffected carriers who had normal levels.

Effects of Mutations on Protein Function

PYCR2 is expressed broadly, including dermal fibroblasts.[14] To study the effect of patient mutations, we obtained skin biopsies, cultured primary skin fibroblasts, then collected whole cell lysates from cultures at early passage from affected individuals and carrier parents from 3 families, representing 3 different mutations (Fig 4). Western blot analysis using a c-terminal PYCR2 antibody demonstrated presence of the full-length protein associated with both missense alleles tested (p.199Arg/Trp and p.232 Cys/Gly), suggesting that the mutations did not appreciably destabilize the protein. As expected, less protein was detected from the parent carrier associated with the truncated allele tested (p.266Arg/Stop) due to the lack of the c-terminal antigen. No protein was detected in the affected individual. As a reference, we included primary skin fibroblasts from a family with *PYCR1* null mutation,[3] in which PYCR2 protein, but not PYCR1 protein, was detected (Fig 4A). We also noted essentially unchanged expression levels of PYCR1 in *PYCR2*-mutated samples, suggesting lack of expression compensation. Interestingly, we noted an upper shadow band on the PYCR1 blot, which, we concluded, likely represents nonspecific binding to PYCR2, because it was absent in the homozygous truncated p.266Stop/Stop sample at the correct molecular weight. Furthermore, the 2 samples harboring the p.266Arg/Stop mutation also showed a band of lower

FIGURE 2: Triangular facial appearance of individuals with *PYCR2* mutations. Typical triangular faces associated with bulbous nasal tip, malar hypoplasia, and prominent low-set ears were observed in most cases. Pedigree number and individual ID with corresponding homozygous mutation are shown.

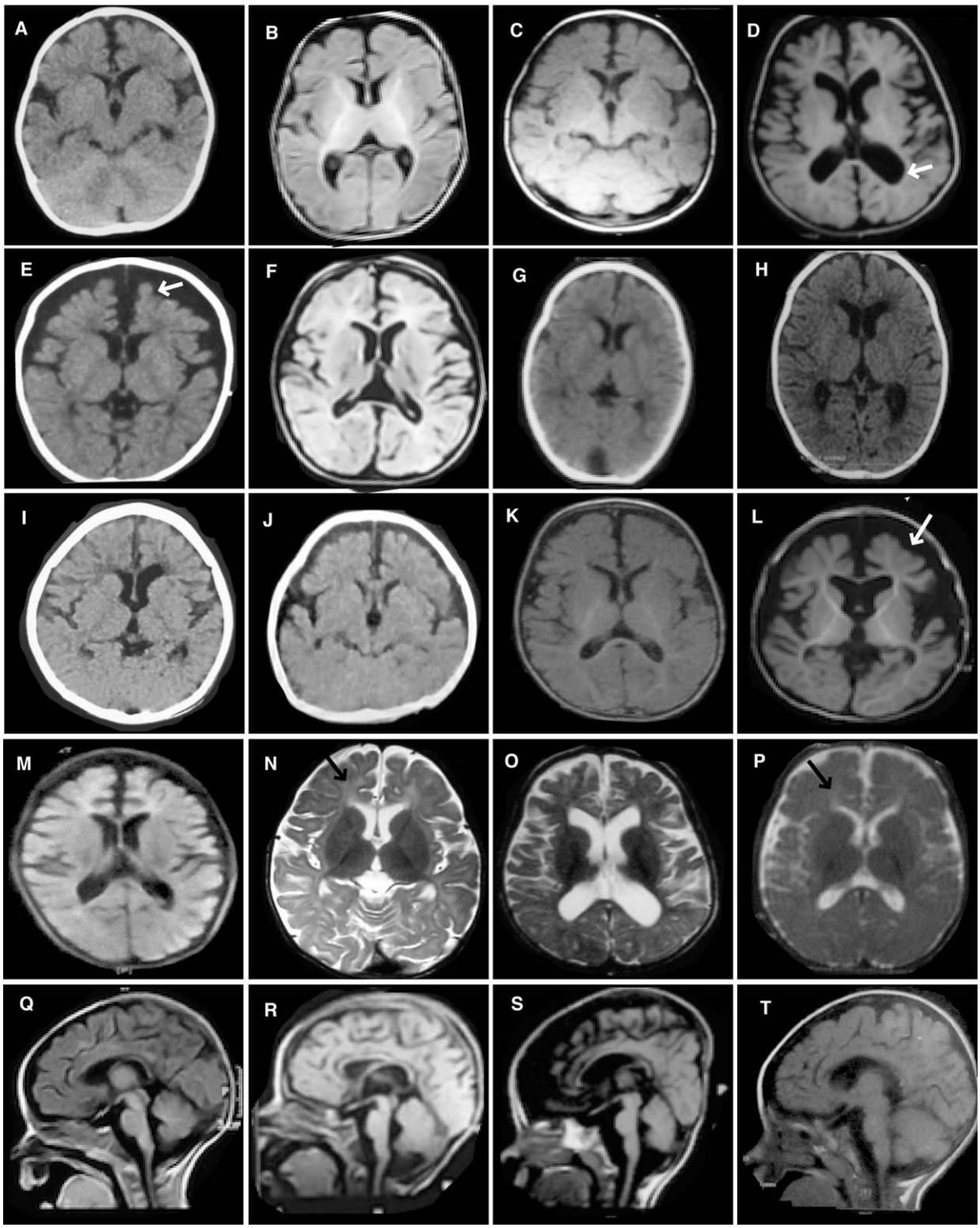

FIGURE 3: Brain imaging of patients with *PYCR2* mutations. Head computed tomography or brain magnetic resonance imaging (MRI) of 13 affected individuals are illustrated: Patients 1232-III-1 (A, age = 12 months), 1232-III-2 (B, Q, age = 10 months), 1240-II-2 (C, N, age = 21 months), 2404-III-7 (D, O, age = 3 years), 2566-IV-2 (E, age = 3 years), 2664-III-1 (F, R, age = 18 months), 2682-III-1 (G, age = 12 months), 2682-III-2 (H, age = 12 months), 2706-III-3 (I, age = 2 years), 2706-III-4 (J, age = 9 months), 3109-III-3 (K, P, age = 18 months), 3740-III-2 (L, S, age = 2 years), 4592-III-3 (M, T, age = 1 year). Axial T1-weighted brain MRI (A–M) demonstrated global brain atrophy, thin corpus callosum, mild cortical atrophy, or severe brain atrophy (*white arrows* in E and L), as well as ventriculomegaly (*white arrow* in D). Axial T2-weighted (N–P) and midline sagittal T1-weighted (Q–T) brain MRI demonstrated hypomyelination with reduced white matter volume (most notable in N, shown by *black arrows*), basal ganglia, pons, and cerebellum were either mildly reduced in size or were within normal limits.

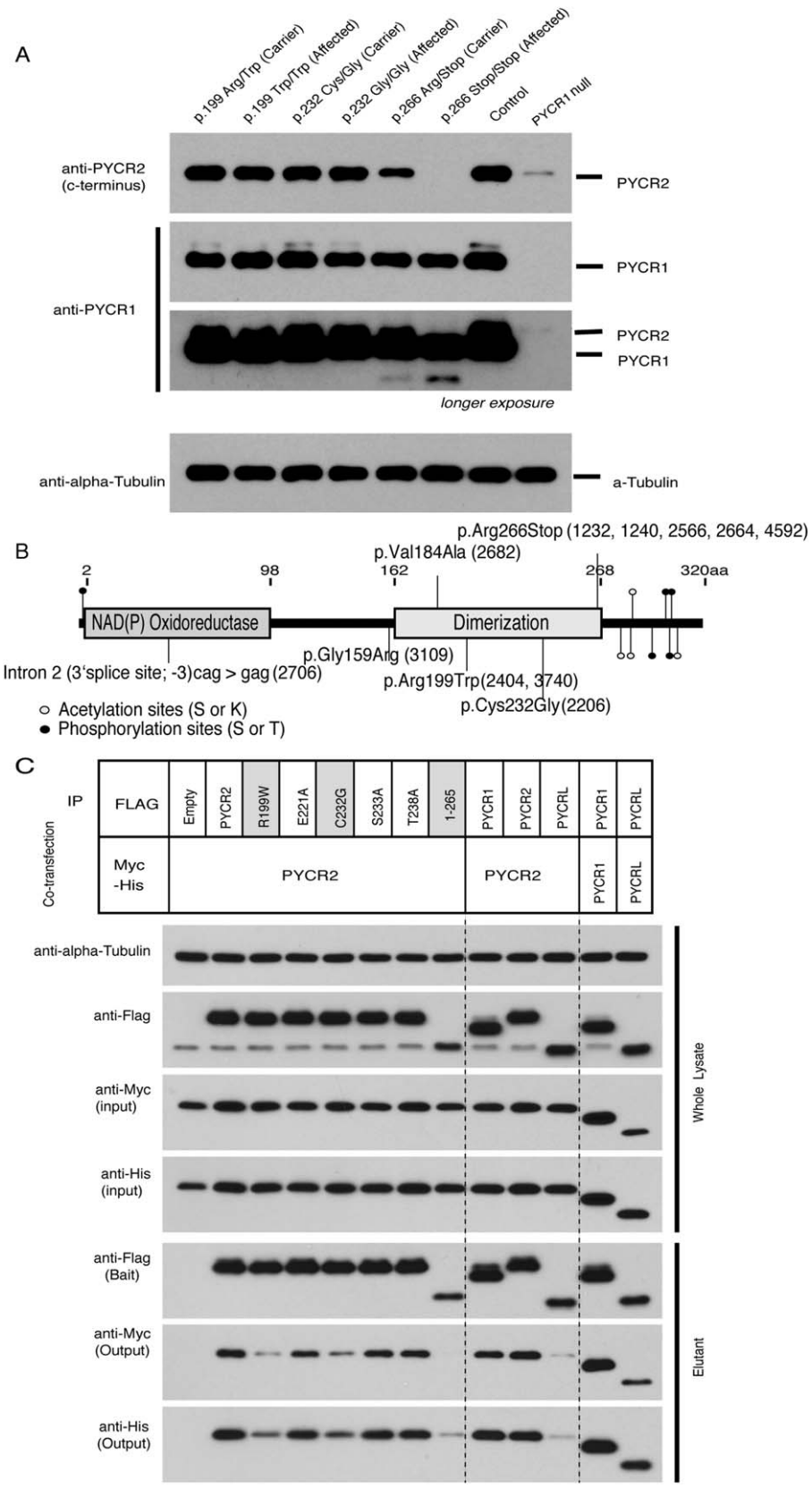
A
p.199 Arg/Trp (Carrier)
p.199 Trp/Trp (Affected)
p.232 Cys/Gly (Carrier)
p.232 Gly/Gly (Affected)
p.266 Arg/Stop (Carrier)
p.266 Stop/Stop (Affected)
Control
PYCR1 null
anti-PYCR2 (c-terminus)
PYCR2
anti-PYCR1
PYCR1
PYCR2
PYCR1
longer exposure
anti-alpha-Tubulin
a-Tubulin
B
p.Arg266Stop (1232, 1240, 2566, 2664, 4592)
p.Val184Ala (2682)
2
98
162
268
320aa
NAD(P) Oxidoreductase
Dimerization
p.Gly159Arg (3109)
Intron 2 (3'splice site; -3)cag > gag (2706)
p.Arg199Trp(2404, 3740)
p.Cys232Gly(2206)
Acetylation sites (S or K)
Phosphorylation sites (S or T)
C
IP
FLAG
Empty
PYCR2
R199W
E221A
C232G
S233A
T238A
1-265
PYCR1
PYCR2
PYCRL
PYCR1
PYCRL
Co-transfection
Myc -His
PYCR2
PYCR2
PYCR1
PYCRL
anti-alpha-Tubulin
anti-Flag
anti-Myc (input)
anti-His (input)
Whole Lysate
anti-Flag (Bait)
anti-Myc (Output)
anti-His (Output)
Elutant

FIGURE 4.

molecular weight of lower intensity upon longer exposure, likely corresponding to the truncated PYCR2 protein. We conclude that the missense mutations tested result in stable protein and that the p.266Arg/Stop mutation results in some retention of mutant truncated protein.

Because missense mutations tested did not disrupt stability of the protein, we tested whether mutations affect function. P5C-reductase family members function as multimers, and family members contain a conserved P5CR-dimerization domain.[15] We thus introduced patient mutations (p.199Arg/Trp, p.232 Cys/Gly, p.266Arg/Stop) into FLAG- or Myc/His-tagged mammalian expression vectors encoding PYCR2 and cotransfected 293T cells with differently tagged expression vectors for coimmunoprecipitation studies. We also included alanine substitutions (p.Glu221Ala, p.Ser233Ala, and p.Thr238Ala) of amino acids that were suggested to be crucial for dimerization based on PYCR1 structure.[15,16] PYCR1 and PYCRL, the two other paralogues, were also included to test dimerization. The cell lysates were subjected to immunoprecipitation using an anti-FLAG affinity gel, and the eluted samples were analyzed by Western blot with antibodies against c-Myc or 6X His (Fig 4C). We found that all the expression vectors produced detectable protein of predicted molecular weight. Wild-type PYCR2 coimmunoprecipitated wild-type PYCR2, as did PYCR2 proteins with the tested alanine mutations, whereas PYCR2 with the patient missense or nonsense mutations showed reduced coprecipitation of wild-type protein. PYCR2 also coprecipitated with PYCR1, but barely with PYCRL, whereas PYCR1 and PYCRL each coprecipitated with itself. We conclude that patient mutations can impair protein multimerization, and that there is potential promiscuity in the association between PYCR paralogue proteins.

Discussion

Expansion of the Clinical Phenotype

In this study, we identified 14 individuals with mutations in the *PYCR2* gene, expanded and refined the clinical presentation, and tested the effects of mutations in primary patient cells and in heterologous cells. Key clinical features noted in all patients included an early presentation of neurodevelopmental delay within the first year of life, secondary microcephaly that became pronounced with age given the progressive neurodegenerative nature of the disease,[17] and characteristic triangular facies, malar hypoplasia, large malformed ears, and upturned bulbous nose (see Supplementary Table). Similar minor dysmorphisms were observed in previously reported patients.[10] We appreciated some variability in facial features, likely due to the varying range of facial muscular atrophy and age of evaluation. Skeletal features of arachnodactyly, long toes, and pectus carinatum observed in 4 patients were not previously reported. In addition, severe muscle wasting, limb hypertonia, brisk reflexes, inability to ambulate, and hyperkinetic extremity movements aided in making the diagnosis.[10]

Although this condition has been classified as a hypomyelinating leukodystrophy, we found that the imaging features were variable, ranging from subtle white matter T2 hyperintensities to progressive brain atrophy. Hypomyelinating leukodystrophies (HLDs) represent a genetically heterogeneous group of neurological disorders characterized by impaired myelin formation in the brain. To date, 11 different genetic forms of HLD have been described with mutations in genes involved in myelin formation and oligodendrocyte maturation.[18] A new term "genetic leukoencephalopathy" was recently coined by the Global Leukodystrophy Initiative Consortium to define inherited disorders that are actually primarily neuronal diseases with secondary hypomyelination, such as Cockayne syndrome, *AGC1*-related disorders, or other genetic conditions with major systemic manifestations,[19] and one could consider that *PYCR2* could be included in this group. The clinical features of early onset intellectual disability, microcephaly, epilepsy, and brain atrophy suggest primary neuronal dysfunction with secondary deficit in myelination, in contrast to most patients with HLD, who often present with cerebellar ataxia, axial hypotonia, spasticity, and nystagmus, without severe diffuse cerebral atrophy.[18]

FIGURE 4: Altered protein levels and impaired dimerization correlate with patient mutations in *PYCR2*. (A) Protein expression in skin fibroblasts from patients (affected) or parents (carrier) with corresponding mutations, using C-terminal PYCR2-specific, PYCR1 (lower with longer exposure), or tubulin antibodies. Parents showed reduced and patients showed absent PYCR2 protein level with p.266R/Stop mutation. The last lane is a lysate of skin fibroblasts from a patient with *PYCR1* null mutation, with absent PYCR1 and little PYCR2. Truncated protein detected in p.266 Stop/Stop lane with longer exposure was evident in the carrier. No compensatory increase in PYCR1 was detected in patient cells. (B) PYCR2 protein domain structure and location of identified mutations. Putative phosphorylation and acetylation are indicated. (C) Impaired multimerization of PYCR2 with the dimerization domain patient mutations. 293T cells were cotransfected with expression vectors encoding FLAG-tagged PYCR2 (wild-type or mutants) or Myc/His-tagged wild-type PYCR2. Cell lysates were subject to coimmunoprecipitation with an anti-FLAG gel. Patient mutations (p.R199W, p.C232G, or truncating p.1–265) are highlighted with gray, and additional mutations predicted to impair multimerization (p.E221A, p.S233A, p.T238A), wild-type PYCR1, and PYCRL were also included. The top 4 blots show protein levels in whole cell lysates (input); the bottom 3 show protein levels in elutants after anti-FLAG immunoprecipitation (output).

During the study course, about half of the cohort of *PYCR2*-mutated patients succumbed from failure to thrive and complications from pulmonary infections, and there were no living survivors beyond the age of 10 years. No specific cause of death has been ascribed that would suggest other organ involvement. In the previous report, none of the patients died and the longest living survivor was 11 years 6 months old.[10] Whether the difference in mortality in our cohort reflects differences in the ascertained patient population, the standard of medical care, the opportunistic infection, or outlier effects remains to be determined.

The Spectrum of PYCR-Related Disorders

The pivotal role of PYCR proteins in proline metabolism, the proximity to the urea and citric acid cycles, and the clinical overlap between *PYCR1* and *PYCR2* mutations underscore the potential myriad of biochemical defects that may result from *PYCR*-family gene mutations. *PYCR1*-related cutis laxa and progeroid syndrome present with the core features of intrauterine growth retardation, wrinkled skin, joint hyperlaxity, and a typical progeroid gestalt.[20] Some of the facial features such as triangular face, bulbous upturned nose, and long philtrum mirror PYCR2-facies, but cutis laxa and progeroid features are missing. Furthermore, *PYCR1* mutations usually associate with milder intellectual disability and can have normal head circumference. Rare associations with *PYCR1* mutations are corneal clouding, cataracts, strabismus, contractures, inguinal hernia, and athetoid movements.[9,20] The abnormal movements described as "stereotypic dystonic and jerky arm movements" are similar to the hyperkinetic movements seen in our cohort. We postulate that *PYCR1*- and *PYCR2*-related disorders are likely a continuum of the same neurodevelopmental disorder due to defect in mitochondrial proline synthesis, wherein cutaneous findings are prominent with *PYCR1* mutations, and patients with *PYCR2* mutations have a severe neurological phenotype. Although PYCRL shares 45% amino acid similarity to the other 2 isoforms, mutations in its gene has not been associated with human disease. Conversely, *ALDH18A1*, encoding the upstream P5CS protein, is mutated in autosomal recessive cutis laxa type IIIA[21] and the autosomal dominant form of progeroid de Barsy-like cutis laxa syndrome,[22] suggesting that PYCR1 and P5CS have a more important role in skin function than *PYCR2*.[6] Another rare finding seen in one-third of our patients was excessive vomiting, which has been reported only in a 12-year-old male with autosomal dominant *ALDH18A1* cutis laxa phenotype.[23]

PYCR2 *Genotype–Phenotype Correlation and Metabolic Profiling*

PYCR2 mutations detected in this study were mostly clustered around the dimerization domain. The variant c.796G>A (p.Arg266*) was the most common mutation, seen in 4 of 12 families, whereas the c.595G>A (p.Arg199Trp) mutation was present in 2 families. The number of families sharing mutations suggests common founder alleles in these populations. Three of the mutations were unique in these families, including a predicted splice site mutation in the family from Pakistan, and none overlaps with published variants. In the current study, truncating mutations in *PYCR2* led to reduced protein levels in fibroblasts. The tested missense mutations showed intact protein levels but failure to multimerize, presumably a requirement for enzymatic activity based upon other studies.[15,24] Of note, 2 of our most severely affected patients (2404-III-7, 3740-III-3) with severe brain atrophy shared a common mutation, p.Arg199Trp, which could indicate a more severe effect on protein function, perhaps interfering with function of other PYCR family proteins through dominant negative activities.

PYCR1 and *PYCR2* are proposed for biosynthesis of proline from glutamate via P5C in the mitochondrial milieu, whereas *PYCRL* is proposed for biosynthesis of proline from ornithine in the cytosol.[25] The reduction of P5C to proline utilizes cofactors NADH/NADPH, hence the isoforms are responsible for shuttling redox equivalents and maintaining an oxidative balance.[26,27] Increasing evidence suggests a correlation of NAD^+-consuming enzymes with neuronal injury mediated via apoptosis-inducing factor and adenosine triphosphate depletion.[28] PYCR isozymes have also been demonstrated to colocalize with the stress response protein RRM2B (ribonucleotide reductase small subunit B) to prevent cellular injury from oxidative stress.[29] Recently, a role for *PYCR2* in cellular apoptosis was suggested in melanoma cells, as *PYCR2* knockdown led to decreased proliferative capacity and activation of AMPK/mTOR-induced autophagy.[19] PYCR2 deficiency led to increased apoptosis under oxidative stress when cells with homozygous frameshift mutations were treated with H_2O_2, and knockdown of *PYCR2* ortholog *pycr1b* in a zebrafish model resulted in smaller head/brain, shorter body, downtilted tail, and hypomotility.[4]

The role of glutamate in neuronal toxicity has also been extensively studied,[30] and could very well be a part of neurological dysfunction cascade due to *PYCR2* mutations. In this study, we did not detect any significant change in plasma amino acids of affected individuals tested. Slightly elevated level of glutamate in urine was

noted in Patients 2206-III-4 and 2664-III-1, which could potentially reflect the upstream accumulation of glutamate, but will require additional studies to confirm. A clear characterization of metabolic derangements in PYCR-related disorders is still lacking, and reports to date fail to find evidence of systemic biochemical derangement.[10,20]

Acknowledgment

This work was supported by the NIH (NICHD P01HD070494, NINDS R01NS048453, J.G.G.; NINDS P30NS047101 for imaging support), the Yale Center for Mendelian Disorders (NHGRI U54HG006504, NINDS RC2NS070477), the Gregory M. Kiez and Mehmet Kutman Foundation, the Simons Foundation (175303, 275275), the Qatar National Research Fund (NPRP 6-1463-3-351, J.G.G.; NHGRI U54HG003067 to the Broad Institute), and a Pilot Grant awarded by the Center for Basic and Translational Research on Disorders of the Digestive System at the Rockefeller University through the generosity of the Leona M. and Harry B. Helmsley Charitable Trust (I.M.-V.).

J.G.G. is an Investigator of the Howard Hughes Medical Institute.

We thank B. Reversade for providing *PYCR1*-mutated fibroblasts; the Yale Biomedical High Performance Computing Center for data analysis and storage; the Yale Program on Neurogenetics and the Yale Center for Human Genetics and Genomics; the Center for Inherited Disease Research for genotyping; the Simons Foundation Autism Research Initiative; and patients and parents for participation.

Author Contributions

M.S.Z., T.S., M.I., L.S., I.G., and G.A.-S. identified patients for study, H.-J.J. performed cell culture and Western blotting, M.S.A.-H. performed Sanger confirmation, G.B., I.M.-V., and E.D. organized clinical data and generated figures, M.S.Z. and J.G.G. supervised the project, and G.B., I.M.-V., M.S.Z., and J.G.G. contributed to the manuscript.

Potential Conflicts of Interest

Nothing to report.

References

1. Elijah A, Leonard F. Metabolism of proline and the hydroxyprolines. Annu Rev Biochem 1980;49:1005–1061.
2. Perez-Arellano I, Carmona-Alvarez F, Martinez AI, et al. Pyrroline-5-carboxylate synthase and proline biosynthesis: from osmotolerance to rare metabolic disease. Protein Sci 2010;19:372–382.
3. Shafqat S, Velaz-Faircloth M, Henzi VA, et al. Human brain-specific L-proline transporter: molecular cloning, functional expression, and chromosomal localization of the gene in human and mouse genomes. Mol Pharmacol 1995;48:219–229.
4. Tadros SF, D'Souza M, Zettel ML, et al. Glutamate-related gene expression changes with age in the mouse auditory midbrain. Brain Res 2007;1127:1–9.
5. Yildirim Y, Tolun A, Tuysuz B. The phenotype caused by PYCR1 mutations corresponds to geroderma osteodysplasticum rather than autosomal recessive cutis laxa type 2. Am J Med Genet A 2011;155A:134–140.
6. Zampatti S, Castori M, Fischer B, et al. De Barsy syndrome: a genetically heterogeneous autosomal recessive cutis laxa syndrome related to P5CS and PYCR1 dysfunction. Am J Med Genet A 2012;158A:927–931.
7. Baumgartner MR, Hu CA, Almashanu S, et al. Hyperammonemia with reduced ornithine, citrulline, arginine and proline: a new inborn error caused by a mutation in the gene encoding delta(1)-pyrroline-5-carboxylate synthase. Hum Mol Genet 2000;9:2853–2858.
8. Guernsey DL, Jiang H, Evans SC, et al. Mutation in pyrroline-5-carboxylate reductase 1 gene in families with cutis laxa type 2. Am J Hum Genet 2009;85:120–129.
9. Reversade B, Escande-Beillard N, Dimopoulou A, et al. Mutations in PYCR1 cause cutis laxa with progeroid features. Nat Genet 2009;41:1016–1021.
10. Nakayama T, Al-Maawali A, El-Quessny M, et al. Mutations in PYCR2, encoding pyrroline-5-carboxylate reductase 2, cause microcephaly and hypomyelination. Am J Hum Genet 2015;96:709–719.
11. DePristo MA, Banks E, Poplin R, et al. A framework for variation discovery and genotyping using next-generation DNA sequencing data. Nat Genet 2011;43:491–498.
12. Dixon-Salazar TJ, Silhavy JL, Udpa N, et al. Exome sequencing can improve diagnosis and alter patient management. Sci Transl Med 2012;4:138ra178.
13. Akizu N, Cantagrel V, Schroth J, et al. AMPD2 regulates GTP synthesis and is mutated in a potentially treatable neurodegenerative brainstem disorder. Cell 2013;154:505–517.
14. Su AI, Wiltshire T, Batalov S, et al. A gene atlas of the mouse and human protein-encoding transcriptomes. Proc Natl Acad Sci U S A 2004;101:6062–6067.
15. Nocek B, Chang C, Li H, et al. Crystal structures of delta1-pyrroline-5-carboxylate reductase from human pathogens Neisseria meningitides and Streptococcus pyogenes. J Mol Biol 2005; 354:91–106.
16. Meng Z, Lou Z, Liu Z, et al. Crystal structure of human pyrroline-5-carboxylate reductase. J Mol Biol 2006;359:1364–1377.
17. Woods CG, Bond J, Enard W. Autosomal recessive primary microcephaly (MCPH): a review of clinical, molecular, and evolutionary findings. Am J Hum Genet 2005;76:717–728.
18. Pouwels PJ, Vanderver A, Bernard G, et al. Hypomyelinating leukodystrophies: translational research progress and prospects. Ann Neurol 2014;76:5–19.
19. Vanderver A, Prust M, Tonduti D, et al. Case definition and classification of leukodystrophies and leukoencephalopathies. Mol Genet Metab 2015;114:494–500.
20. Dimopoulou A, Fischer B, Gardeitchik T, et al. Genotype-phenotype spectrum of PYCR1-related autosomal recessive cutis laxa. Mol Genet Metab 2013;110:352–361.
21. Skidmore DL, Chitayat D, Morgan T, et al. Further expansion of the phenotypic spectrum associated with mutations in ALDH18A1,

encoding Δ^1-pyrroline-5-carboxylate synthase (P5CS). Am J Med Genet A 2011;155A:1848–1856.

22. Fischer-Zirnsak B, Escande-Beillard N, Ganesh J, et al. Recurrent de novo mutations affecting residue Arg138 of pyrroline-5-carboxylate synthase cause a progeroid form of autosomal-dominant cutis laxa. Am J Hum Genet 2015;97:483–492.
23. Nozaki F, Kusunoki T, Okamoto N, et al. ALDH18A1-related cutis laxa syndrome with cyclic vomiting. Brain Dev 2016; doi:10.1016/j.braindev.2016.01.003.
24. Meng Z, Lou Z, Liu Z, et al. Purification, characterization, and crystallization of human pyrroline-5-carboxylate reductase. Protein Expr Purif 2006;49:83–87.
25. De Ingeniis J, Ratnikov B, Richardson AD, et al. Functional specialization in proline biosynthesis of melanoma. PLoS One 2012;7:e45190.
26. Merrill MJ, Yeh GC, Phang JM. Purified human erythrocyte pyrroline-5-carboxylate reductase: preferential oxidation of NADPH. J Biol Chem 1989;264:9352–9358.
27. Mixson AJ, Phang JM. The uptake of pyrroline 5-carboxylate. Group translocation mediating the transfer of reducing-oxidizing potential. J Biol Chem 1988;263:10720–10724.
28. Ying W. NAD+ and NADH in neuronal death. J Neuroimmune Pharmacol 2007;2:270–275.
29. Kuo ML, Lee MB, Tang M, et al. PYCR1 and PYCR2 interact and collaborate with RRM2B to protect cells from overt oxidative stress. Sci Rep 2016;6:18846.
30. Sheldon AL, Robinson MB. The role of glutamate transporters in neurodegenerative diseases and potential opportunities for intervention. Neurochem Int 2007;51:333–355.